MEMBRANE INTERACTIONS IN NERVE MYELIN:

II. Determination of Surface Charge from Biochemical Data

HIDEYO INOUYE AND DANIEL A. KIRSCHNER
Department of Neuroscience, Children's Hospital, and Department of Neuropathology, Harvard Medical School, Boston, Massachusetts 02115

ABSTRACT In our accompanying paper (Inouye and Kirschner, 1988) we calculated the surface charge density at the extracellular surfaces in peripheral and central nervous system (PNS; CNS) myelins from observations on the dependency of the width of the extracellular space on pH and ionic strength. Here, we have determined the surface charge density of the membrane surfaces in myelin from its chemical composition and the localization of some of its molecular components. We then analyzed the attractive and repulsive forces between the apposed surfaces and calculated equilibrium periods for comparison with the measured values.

The biochemical model accounts for the observed isoelectric range of the myelin period and, with the surface charge reduced (possibly by divalent cation binding or a space charge approximation), the model also accounts for the dependency of period on pH above the isoelectric range. At the extracellular (and cytoplasmic) surfaces the contribution of lipid (with pI ~2) to the net surface charge is about the same in both PNS and CNS myelin, whereas the contribution of protein depends on which ones are exposed at the two surfaces. The protein conformation and localization modulate the surface charge of the lipid, resulting in positively-charged cytoplasmic surfaces (pI ~9) and negatively-charged extracellular surfaces (pI ~2–4). The net negative charge at the extracellular surface is due in CNS myelin to lipid, and in PNS myelin to both lipid and (P0) glycoprotein. The net positive charge at the cytoplasmic surface is due in CNS myelin mostly to basic protein, and in PNS myelin to P0 glycoprotein and basic protein. The invariance of the cytoplasmic packing may be due to specific short-range interactions. Our models demonstrate how the particular myelin proteins and their localization and conformation can account for the differences in inter-membrane interactions in CNS and PNS myelins.

INTRODUCTION

In the accompanying paper (Inouye and Kirschner, 1988) we report the pH and ionic strength dependence of the widths of the inter-membrane spaces in peripheral and central nervous system (PNS; CNS) myelins. We found that the extracellular separation varied systematically as a function of pH and ionic strength, while the cytoplasmic separation was essentially invariant. We used these measurements of myelin period and inter-membrane spaces to determine the surface charge density on the extracellular membrane surfaces. Here, we have modeled the extracellular and cytoplasmic leaflets from the known biochemical composition of myelin and the inferred localization of components. We have then determined to what extent this chemical model is in agreement with the observed surface charge density.

From the density and composition of myelin, we estimated the molar ratios of its components. The lipids were assigned to either the cytoplasmic or extracellular leaflet of the membrane and basic protein was assigned to the cytoplasmic side (Kirschner et al., 1984; Gwarsha et al., 1984). The conformation of proteolipid protein (PLP) in the CNS and of (P0) glycoprotein in the PNS and their domains in the cytoplasmic and extracellular spaces between the apposed membranes were as proposed from their primary structures (Laursen et al., 1984; Stoffel et al., 1984; Lemke and Axel, 1985). Given the pK's, amounts, and membrane sidedness of the ionizable groups, and the pH and ionic strength of the immersion medium, we then estimated the net surface charge density at each side of the membrane. Such modeled membrane surfaces are consistent with the observed isoelectric range of the myelin period and, with the surface charge reduced, also are consistent with the dependency of period on pH above the isoelectric range. Preliminary reports of some of this work have been presented (Inouye and Kirschner, 1986a, b).

Please address all correspondence to Dr. Daniel A. Kirschner, Department of Neuroscience, Children's Hospital, 300 Longwood Avenue, Boston, MA 02115.

METHODS OF ANALYSIS

To account for the pH- and ionic strength-dependent changes in membrane separation, we first derived a structural model for the distribution

of lipids and proteins in the two leaflets of the myelin membrane. Then, given the molar content and pK values of the ionizable groups on the membrane surfaces, we calculated the surface charge density, electrostatic repulsion, and the equilibrium separation or period (Ninham and Parsegian, 1971).

Biochemical Data and Localization of Components

The numbers of lipid and protein molecules were determined from the available data for isolated myelin which has been summarized in recent reviews (Norton and Cammer, 1984; Lees and Brostoff, 1984). The purity of isolated myelin is usually based on its electron microscopic appearance which ideally should be a multilamellar membrane system free of contaminating membranes associated with either other organelles or with the cytoplasm-containing regions of myelin (i.e., paranodal region and Schmidt-Lanterman incisures; see Norton and Cammer, 1984). Notwithstanding the accepted criterion for the purity of isolated myelin, we have found considerable variability of composition in the myelin biochemical literature. The dispositions of the lipids were determined from the chemical (Gwarsha et al., 1984; Linington and Rumsby, 1980) and structural (Caspar and Kirschner, 1971; Worthington, 1971; Kirschner and Ganser, 1982) data. The protein disposition was determined from the proposed conformation for proteolipid protein in CNS myelin (Laursen et al., 1984; Stoffel et al., 1984) and for P0-glycoprotein in PNS myelin (Lemke and Axel, 1985). Myelin basic protein was assigned to the cytoplasmic surface (reviewed by Kirschner et al., 1984). The lipid and protein composition of myelin, and the localization of the molecular components to the two halves of the membrane are summarized in Tables I–VI.

Calculating Membrane Surface Charge Density

The fixed surface charge density, σ, is determined by the chemical composition of the membrane, while the extent of the ionization is due to the proton dissociation constant and the local proton concentration. The surface charge of the membrane is

$$\sigma = eN/S, \tag{1}$$

where e is the elementary charge and N is the number of fixed charges in the surface area S. When there are ionizable groups A and B, the proton dissociation is described as

$$\begin{aligned} HA &\rightleftharpoons A^- + H^+ \\ BH^+ &\rightleftharpoons B + H^+. \end{aligned} \tag{2a}$$

The apparent proton dissociation constants K_a and K_b are described according to the mass action law,

$$\begin{aligned} K_a &= [A^-][H^+]/[HA] \\ K_b &= [B][H^+]/[BH^+], \end{aligned} \tag{2b}$$

where $[H^+]$ is the measured proton concentration in the bulk medium. Since the proton concentration follows the Boltzmann distribution under an electrostatic potential field $\phi(x)$, then

$$[H_x^+] = [H^+] \exp[-e\phi(x)/kT], \tag{3a}$$

where $[H_x^+]$ is the proton concentration at position x under an electric field $\phi(x)$, k is the Boltzmann constant and T is the absolute temperature.

Thus, for an ionizable group at the surface, the apparent pK (= $-\log$ K) is related to the intrinsic pK (pK_{int}) by

$$pK = pK_{int} - e\phi(x_s)/(2.303\,kT). \tag{3b}$$

For example, for a net negatively-charged surface, $\phi(x_s) < 0$, so the apparent pK is actually greater than the intrinsic pK, while for a net positively-charged surface, $\phi(x_s) > 0$, so pK < pK_{int}. With the type of dissociation described by Eq. 2, the surface charge density given by Eq. 1 becomes

$$\sigma = (e/S)\left(-\sum_i A_i^- + \sum_j BH_j^+\right). \tag{4}$$

From the condition that diffusable counterions neutralize the surface charges, the surface charge density σ of the isolated membrane is given by

$$\sigma = (\epsilon kT/2\pi e)\,\kappa \sinh[e\phi(x_s)/2kT], \tag{5}$$

where κ is the Debye parameter equal to $[8\pi e^2 n/(\epsilon kT)]^{1/2}$, ϵ is the dielectric constant of the medium and n is the concentration of the univalent electrolyte (Verwey and Overbeek, 1948). The surface potential and surface charge density are obtained from Eqs. 1 or 4, and 5, given the molar content and proton dissociation of the ionizable groups, the pH, and the concentration of the electrolytes in the medium. When the intervening medium contains divalent cations and the surface potential is small, a concentration n of electrolyte is substituted for by the value of the ionic strength (i.e., by $\Sigma_i\ 0.5 n_i z_i^2$) in the Debye parameter κ.

We determined the surface charge of the lipids and proteins, and that of the net composition for each membrane leaflet (at an ionic strength of 0.06) by systematically varying the value of $\phi(x_s)$ (in increments of 1 mV) in Eqs. 4 and 5 and searching for the closest agreement between the calculated values of σ from these two equations. Note that the net surface charge for a membrane leaflet is not equal to the summation of the charges for the individual constituents for that surface since, according to Eqs. 2b and 3a, the inclusion of additional constituents influences the electrostatic potential and the dissociation of the ionizable group.

Calculating Myelin Periods

At the equilibrium myelin period the van der Waals attractive force is balanced against the repulsion forces. We searched for the equilibrium periods by systematically increasing the period in steps of 1 Å from an initial value equal to the exclusion length of the membrane pair (138 Å for PNS and 123 Å for CNS myelin; see accompanying paper), calculating the van der Waals attraction force, electrostatic repulsion force and

TABLE I
PERCENT WEIGHT CONTENT OF PROTEIN, LIPID AND WATER IN MYELIN

	ρ*	W_{water}‡	$W_{protein}$§	W_{lipid}§
CNS	1.10 (.02)	45	25.4 (4.1)	74.6 (4.1)
PNS	1.07	45	26.4 (4.1)	73.6 (4.1)

*Myelin from rat brain bands in a sucrose gradient at 0.65 M (1.08 g/cm^3) (Norton and Cammer, 1984) and 0.67 M (1.086 g/cm^3) (Waehneldt, 1978) and in a CsCl gradient at 0.85 M (1.11 g/cm^3) (Norton and Cammer, 1984). For the density of CNS myelin we took the average of the values for the two different gradient systems. Myelin from rabbit sciatic nerve bands in a sucrose gradient at 0.57 M (1.07 g/cm^3) (Linington et al., 1980; Matthieu et al., 1979).

‡The value, given as a weight fraction of hydrated myelin, is in the 30–50% range estimated from x-ray diffraction measurements (Schmitt et al., 1941; Finean, 1957; Caspar and Kirschner, 1971; Kirschner and Caspar, 1975).

§The CNS data are averaged values for the rat (Smith, 1968; Norton and Cammer, 1984). The PNS data are values averaged for human, monkey, bovine, and rabbit (cited in Norton and Cammer, 1984).

TABLE II
LIPID COMPOSITION OF MYELIN

Lipid	Mol wt*	CNS‡	PNS§	PNS,shi‖
		weight fraction of total lipids¶		
Cholesterol	387	26.5 (0.9)	27.2 (2.5)	25.6
Cerebroside	805	26.3 (2.6)	15.8 (4.4)	16.9
Sulfatide	894	7.7 (0.6)	5.7 (2.3)	6.8
PE	749	17.0 (0.3)	17.7 (1.4)	18.9
PC	772	10.7 (0.6)	10.0 (1.1)	11.8
PS	811	6.8 (0.6)	11.4 (1.4)	10.8
PI	777	1.3 (0.3)	2.7 (0.3)	2.7
Sphingomyelin	777	3.1 (0.7)	8.8 (0.9)	7.0

*Molecular weights were calculated for cholesterol from its formula and for the other lipids from the data in O'Brien and Sampson (1965).
‡Average values for rat (Smith, 1968; Norton and Cammer, 1984).
§Values for rat (Smith and Curtis, 1979).
‖Values obtained by multiplying the lipid content of rat PNS myelin by the ratio of lipids in shiverer peripheral nerve (Inouye et al., 1985). PE, phosphatidylethanolamine; PC, phosphatidylcholine; PS, phosphatidylserine; PI, phosphatidylinositol.
¶The values in parentheses are the maximum deviations from the mean values.

hydration force, and finding that value of the period which balanced the attractive and repulsive forces.

To test the structural models which are based on biochemical data we compared the calculated with the observed periods as a function of pH and ionic strength. We could also have made the comparison between the calculated surface charge density based on the chemical modeling and that calculated from the observed periods (accompanying paper, Inouye and Kirschner, 1988).

RESULTS AND INTERPRETATION

Molecular Models for CNS and PNS Myelin

Estimated Number of Lipid and Protein Molecules. The number of components in a given volume of myelin was estimated from both chemical and structural data. We defined our unit volume V as containing one molecule of integral membrane protein (PLP for CNS, P0-glycoprotein for PNS) plus lipids and water. This volume is equivalent to $Sd/2$ where S is the surface area of the membrane and d is the myelin period determined from x-ray diffraction. Assuming that the density of the myelin in V is the same as the bulk density of myelin ρ, then the surface area S is determined from the weight fraction and molecular weight of PLP and P0. The number of the i^{th} molecular species N_i is thus described as

$$N_i = (Sd/2)\,\rho w_i 0.602/MW_i, \qquad (6)$$

where MW_i is the molecular weight of the i^{th} component, and w_i is the weight fraction of the i^{th} component in wet myelin.

The content of water (W_{water}) is given as a weight fraction of hydrated myelin, W_{lipid} and $W_{protein}$ are given as weight fractions of dry myelin, $W_{i,lipid}$ is given as weight percent of total lipids, and $W_{i,protein}$ is given as weight percent of total protein. The weight fractions of the individual protein and lipid components, $w_{i,protein}$ and $w_{i,lipid}$,

TABLE III
PROTEIN COMPOSITION OF RODENT CNS MYELIN

	HMW	Wolfgram	Protein*		MBP			
			PLP	DM-20				
MW‡ (kDa)	>60	42–50	29.9	20.5	21.5	18.5	17	14.1
Range§	15–25	2–17	24–52	3–7	0.9	7.7–18.7	2.5	14–38
n	3	7	9	6	1	9	1	9
Average‖	19 (6)	9 (8)	33 (19)	5 (2)	1 —	13 (5)	3 —	26 (12)
Model¶	—	—	49 (27)		— —	17 (7)	— —	34 (16)

*HMW, higher molecular weight proteins, e.g., MAG (myelin associated glycoprotein) with a molecular weight ~100 kDa and consituting ~1% of the total myelin protein (Quarles et al., 1983); cytochemical evidence for MAG localization is conflicting (Webster et al., 1983; Trapp et al., 1984). Wolfgram protein, has a similar amino-acid content as CNP (2',3'-cyclic nucleotide 3'-phosphohydrolase), which is a myelin-associated enyzme of unknown function. PLP, proteolipid protein, the major integral membrane protein of CNS myelin. DM-20, referred to as "intermediate protein" (Morell et al., 1972) or as "Agrawal protein" (Zgorzalewicz et al., 1974), is antigenically and chemically related to PLP (Lees and Brostoff, 1984). There are four antigenically-related species of basic protein in rodent myelin (Barbarese et al., 1978). The 18.5 kDa MBP has been referred to as large or slow-migrating basic protein, and the 14 kDa MBP has been referred to as small or fast-migrating basic protein.
‡The molecular weights are either the apparent Mr from SDS gels, or the value calculated from the primary sequences of the proteins: PLP, Laursen et al. (1984) and Stoffel et al. (1984); 18.5 kDa MBP, Carnegie and Moore (1980) for human; 14 kDa MBP or Pr, Carnegie and Moore (1980) for rat.
§Each protein is listed as a weight fraction of the total protein. The considerable range is based on different quantitative results obtained by densitometry of gels stained with Coomassie blue, amido black, or fast green (Greenfield et al., 1971; Morell et al., 1972; Morell et al., 1973; Zgorzalewicz et al., 1974), or radioimmunoassay (Barbarese et al., 1978; Trotter et al., 1981). *n* is the number of literature values found.
‖Mean value of the range with maximum deviation from mean in parentheses.
¶In the present model PLP, DM-20 and the basic proteins were considered to be the only protein components present in compact myelin. The tabulated values are the mean values for these proteins normalized to 100%.

TABLE IV
PROTEIN COMPOSITION OF RODENT PNS MYELIN

	Protein*					
	HMW	PO(+Y)	X	P1	P_r	P2
MW‡ (kDa)	>60	24.8	19–23	18.5	14.1	15
Range§	14–15	19–71	5–26	2–7	4–12	1
n	2	9	6	6	7	1
Average‖	14	51	14	5	10	1
	(1)	(32)	(12)	(3)	(6)	—
Model¶	—	82		6	12	—
		(56)		(4)	(7)	—

*HMW, higher molecular weight proteins. P0, the major integral membrane glycoprotein of PNS myelin. Y, the oxidized form of P0. X, referred to as "intermediate" or "Agrawal protein" (Zgorzalewicz et al., 1974), and possibly corresponding to degradation products of P0 (Lees and Brostoff, 1984). P1 and P_r, the two major myelin basic proteins of PNS myelin in rodents, identical to the 18.5 and 14 kDa MBPs of CNS myelin; P_r was originally called P2 basic protein. P2, a basic protein found predominantly in PNS myelin, particularly in vertebrates higher than rodents, and not antigenically related to the MBPs.

‡The molecular weights are either the apparent Mr from SDS gels, or the value calculated from the primary sequences of the proteins: P0, Lemke and Axel (1985); P2 or 14.8 kDa MBP, Kitamura et al. (1980) for bovine PNS.

§Each protein is listed as a weight fraction of the total protein. The considerable range is based on quantitation by densitometry of gels stained with Coomassie blue or fast green, or by radioimmunoassay (Greenfield et al., 1973; Zgorzalewicz et al., 1974; Wiggins et al., 1975; Micko and Schlaepfer, 1978; Smith and Curtis, 1979; Greenfield et al., 1980; Weise et al., 1983; Nunn and Mezei, 1984). *n* is the number of literature values found.

‖Mean value of the range with maximum deviation from mean in parentheses.

¶In the present model P0 + X and the basic proteins were considered to be the only protein components present in compact myelin. The tabulated values are the mean values for these proteins normalized to 100%.

is written as

$$w_{i,protein} = W_{i,protein} \times W_{protein} \times (1 - W_{water})$$
$$w_{i,lipid} = W_{i,lipid} \times W_{lipid} \times (1 - W_{water}). \quad (7)$$

The weight contents of water, and the total protein and lipid content of dry myelin are shown in Table I, and the lipid composition data are summarized in Table II. The reported values for the weight content of protein from rodents (mouse and rat) show a large, unexplained variation; however, for our models we chose to average the reported protein contents (Tables III and IV).

Based on biochemical measurements and immunocytochemical observations, we have assumed that the major proteins of multilamellar myelin in the internode are myelin basic protein (MBP) and P0 in the PNS, and MBP and PLP in the CNS. The "intermediate" proteins such as DM-20 in the CNS and X-protein in the PNS are chemically related to PLP and P0 (Lees and Brostoff, 1984), and are assumed to be in multilamellar myelin. We did not include proteins that are associated primarily with the loose membranes bordering compact myelin, or whose localizations are either not known or not agreed upon.

TABLE V
NUMBER OF PROTEIN AND LIPID MOLECULES* AND LIPID DISPOSITION‡

	CNS Myelin			PNS Myelin§		
	Protein	N_i		Protein	N_i	
	PLP and DM-20	1.0		P0 and X	1.0	
	18.5 K MBP	0.55		P1	0.10	
	14 K MBP	1.45		P_r	0.26	
Lipid¶	N_i	CYT	EXT	N_i	CYT	EXT
cholesterol	128	42	86	61	20	41
cerebroside	61	0	61	17	0	17
sulfatide	16	0	16	6	0	6
PE	42	26	16	20	12	8
PC	26	11	15	11	5	6
PS	15	12	3	12	10	2
PI	3	2	1	3	2	1
sphingomyelin	7	3	4	10	5	5
water	11,380			5,337		
Surface area, Å^2	8,816			3,724		
Density, g/cm^3	1.10			1.07		
Period, Å	156			178		

*The number of molecules (N_i) was calculated using the data in Tables I–IV and Eq. 6 assuming one molecule of integral membrane protein (PLP in CNS myelin, and P0 in PNS myelin) per unit surface area.

‡The disposition of the lipids in the cytoplasmic (CYT) and extracellular (EXT) membrane leaflets was based on previous studies: cholesterol, Caspar and Kirschner (1971); glycolipids cerebroside and sulfatide, Linington and Rumsby (1980); PE, averaged from Kirschner and Ganser (1982) and Gwarsha et al. (1984); and PC, PS, PI, and sphingomyelin, Gwarsha et al. (1984). (According to Worthington (1971), Scott et al. (1980), and Allt et al. (1985), cholesterol may be localized equally to both membrane surfaces; however, the electrostatic repulsion would not be affected since cholesterol does not carry ionizable groups.)

§For shiverer PNS myelin (data not shown), in which the basic protein is missing and the lipid composition is altered, the weight contents of the total protein and lipids were assumed the same as in wildtype PNS myelin. The calculated surface area was 2,979 Å^2.

‖The intrinsic pK's of the ionizable groups on the lipids, which contribute to the membrane surface charge density (Fig. 2) were: phosphate, 1.40; carboxyl, 2.21; amino groups, 9.15 (from those of alpha-glycerophosphoric acid and L-serine in bulk solution [Seimiya and Ohki, 1973]). These values are similar to the reported pK's for phosphatidylglycerol (1.2 in Sacre and Tocanne, 1977) and phosphoserine (2.65 for carboxyl and 9.99 for amino in Cevc et al., 1981). The pK_{int} of the sulfate group of sulfatide was assumed to be the same as that of sulfuric acid (1.92). The trimethylamino group of PC was assumed to be completely ionized throughout the pH range.

Disposition of the Lipids and Proteins. Assignment of specific lipids to the cytoplasmic and extracellular leaflets was based on previous studies utilizing lipolytic enzymes (Gwarsha et al., 1984), carbohydrate-specific labels (Linington and Rumsby, 1980), and x-ray diffraction (Caspar and Kirschner, 1971; Kirschner and Ganser, 1982). We calculated the number of the individual lipid

molecules at each surface of the membrane relative to one molecule of integral myelin protein (Table V).

The disposition of the amino acids for the transmembrane, intrinsic myelin proteins (PLP in the CNS and P0-glycoprotein in the PNS) was taken as proposed (Laursen et al., 1984; Stoffel et al., 1984; Lemke and Axel, 1985; see Fig. 1). Two differing conformations have been suggested for PLP. In the Laursen model the acidic residues (Glu, Asp) and basic residues (Arg, Lys) are at comparable amounts at the extracellular surface, whereas in the Stoffel model there are nearly twice as many basic as acid residues at the extracellular surface. The extrinsic myelin basic protein was assigned to the cytoplasmic surface (reviewed in Kirschner et al., 1984). Based on this disposition of proteins, Table VI lists the number of ionizable amino acid residues at each surface of the membrane and the intrinsic pK's for the residues. The hydrophobicity profiles (see also Weise, 1985) and charge distributions of the proteins (Fig. 1) indicate the surface localization of the charges which contribute to the electrostatic repulsion between membranes.

Calculated Surface Charge Density

From the disposition of ionizable lipid and protein groups in myelin, and knowing the pK for these groups, the net charge of the membrane surface as a function of pH under constant ionic strength (0.06) was calculated.

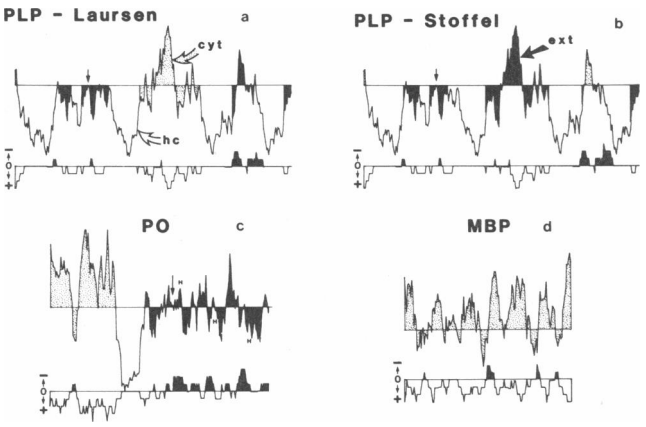

FIGURE 1 Hydropathic profiles (upper curve in each pair) and charge distributions at pH 7 (lower curve in each pair) of the major myelin proteins: (*a*) CNS proteolipid protein, Laursen model; (*b*) CNS proteolipid protein, Stoffel model; (*c*) PNS P0 glycoprotein; (*d*) 18.5 kDa myelin basic protein (MBP). The hydropathic profiles were calculated using the index of Eisenberg et al. (1984); a running average of nine residues was used for both calculations. Cytoplasmic (*dotted*), hydrophobic (*unfilled*), and extracellular (*filled*) domains of the proteins are in accordance with either the proposed conformations for PLP (Laursen et al., 1984; Stoffel et al., 1984, 1985) and P0 (Lemke and Axel, 1985) or with localization studies for MBP (reviewed in Kirschner et al., 1984). The Cooh-terminus of the protein is on the left. The arrows in *a–c* indicate the approximate positions of the covalently-linked fatty acid in PLP (*a, b*) and the oligosaccharide in P0 (*c*). The positions of the three histidine residues in the extracellular domains of P0 are marked by "H". These histidines may be involved in the postulated conformation changes of P0 which could underlie some of the discontinuous structural transitions around neutral pH.

Cytoplasmic Surface. The calculated charge density was positive in both CNS and PNS myelins for pH < 9 (Fig. 2 and Table VII) due to the large amount of positive charge on both myelin basic protein (pI ~ 12) and on the postulated cytoplasmic domains of PLP (pI ~ 10 with either the Laursen or Stoffel model) and of P0 (pI ~ 11). In CNS myelin, the basic protein contributes most of the positive charge, whereas in the PNS, P0 has more positive charge than basic protein but both proteins still contribute substantially. The positive charge from the protein more than offsets the negative charge from the lipid (pI ~ 2) in the cytoplasmic surface.

Extracellular Surface. The calculated charge density was negative in CNS myelin for pH > 2–3 and in PNS myelin for pH > 4 (PNS) (Fig. 2 and Table VII). In CNS myelin the net charge depends on the particular PLP conformation used, with the calculated PLP pI ~ 7 for the Laursen model and ~11 for the Stoffel model. Thus, at neutral pH, the Laursen model predicts twice as much net negative charge on the surface as does the Stoffel model. In either case, the large negative charge on the lipid (pI ~ 2) offsets the lesser positive contribution from protein. In PNS myelin, both P0 (pI ~ 5) and lipid (pI ~ 2) contribute to the large net negative surface charge.

In shiverer PNS myelin the calculated isoelectric point of the cytoplasmic surface was slightly less than that of normal PNS myelin due to the absence of basic protein (Fig. 2), whereas the pI of the extracellular surface showed no significant change, even with an enrichment of the negatively-charged sulfatide lipids in this leaflet (Table VII; Inouye et al., 1985).

Comparison of Calculated and Measured Periods

Using the surface areas determined from the models (Table V), we calculated the myelin periods as a function of pH at ionic strength 0.06 (see Methods of Analysis above). These changes in period predominantly reflect changes in membrane packing at the extracellular apposition (see Table I of the accompanying paper). Although we can also model the cytoplasmic surface and calculate membrane separations at this apposition, the calculated values cannot be compared with the experiment since this apposition has a nearly constant width with pH and ionic strength. Our comparisons between calculated and observed values, then, deal with the extracellular surface.

The myelin periods calculated as a function of pH generally were in agreement with the observed values (Fig. 3), particularly around the isoelectric range. Above this region, however, the calculated period was appreciably greater than the observed values for both CNS and PNS

TABLE VI
NUMBER AND DISPOSITION OF CHARGED AMINO ACID RESIDUES

Group	pK_{int}*	PLP‡ Laursen CYT	PLP‡ Laursen EXT	PLP‡ Stoffel CYT	PLP‡ Stoffel EXT	P0 CYT	P0 EXT	MBP 14K CYT	MBP 18.5K CYT
α-carboxyl	3.8	1	0	1	0	1	0	1	1
Asp (carboxyl)	4.0	2	2	0	3	3	11	7	10
Glu (carboxyl)	4.4	1	6	2	3	3	6	1	1
His (imidazole)	6.3	4	2	0	4	2	3	5	7
α-amino	7.5	0	1	0	1	0	1	0‖	0‖
-SH (thiol)§	9.5	3	0	0	0	1	0	0	0
Tyr (phenol)	9.6	2	3	2	2	3	7	2	4
Lys (ε-amino)	10.4	7	5	4	7	12	6	7	12
Arg (guanidyl)	12.0	5	2	1	6	9	5	17	19
sialic acid¶	4.75	—	—	—	—	0	1	—	—
Molecular weight**		29,903		29,765		24,792		14,079	18,459
Number of residues		276		276		219		127	170
pI‡‡		9.4		9.2		9.6		11.8	11.4

*Intrinsick pK's were values for small molecules dissolved in water (Nozaki and Tanford, 1967).

‡The recently determined primary sequence for rat brain PLP (Milner et al., 1985) does not differ significantly from the sequence for bovine brain PLP which was used in our model.

§Since Lemke and Axel (1985) did not comment on the two cysteine residues in the extracellular domain of P0, these were assumed to be in a disulfide linkage.

‖The N-terminal residues of the basic proteins are acetylated (Carnegie and Moore, 1980; Kitamura et al., 1980).

¶The carbohydrate covalently bound to P0 contains one sialic acid and is located at the extracellular surface (Ishaque et al., 1980). The pK_{int} was assumed to be the same as that for acetic acid.

**Molecular weights were calculated from the reported primary sequences. Post-translational modifications of residues such as by acylation, methylation, phosphorylation, and sulfhydryl linkage were not considered here. The 88th residue of PLP was not determined in Stoffel's model; for the hydropathic profile and charge distribution calculations (Fig. 1), a tyrosine was assumed for this residue. Except for P0 the calculated molecular weights are nearly the same as the apparent molecular weights from SDS polyacrylamide gels.

‡‡The total pI for each protein was calculated from its amino acid composition using the Linderstrøm-Lang equation (cited in Nozaki and Tanford, 1967); the protein was assumed to be dissolved in physiological saline (ionic strength 0.16) at 20°C. The calculated net pI values for PLP and for basic protein were consistent with measured values 9.2–10 or more for PLP (Draper et al., 1978; Thomas and Minassian-Saraga, 1976; Althaus et al., 1983; Feinstein and Felsenfeld, 1975) and pI > 10.5 for basic protein (Althaus et al., 1983).

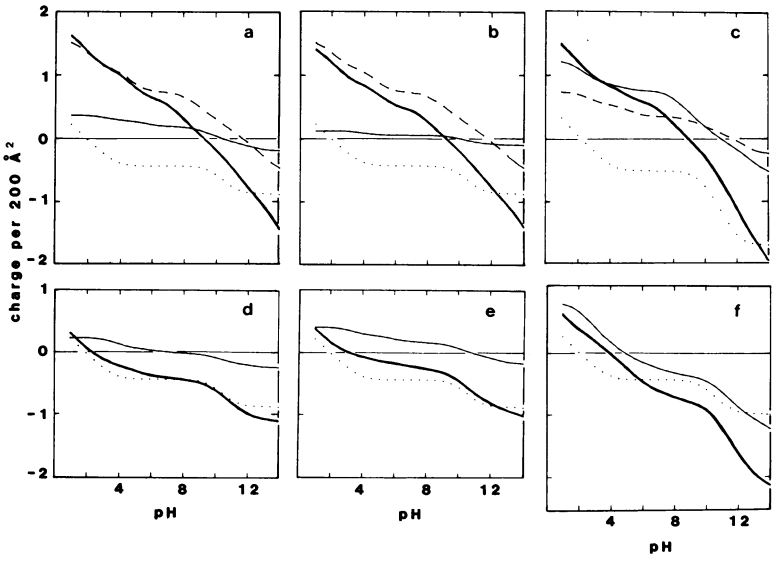

FIGURE 2 Calculated charge density as a function of pH at constant ionic strength 0.06 for cytoplasmic (*upper curves*) and extracellular (*lower curves*) membrane surfaces of CNS (*a, b, d, e*) and PNS (*c, f*) myelins. The contribution of the lipids (*dotted*) and of the individual proteins (MBP, *dashed line*; PLP and P0, *thin lines*), and the net pH (*thick lines*) are indicated. The Laursen model for PLP is shown in *a* and *d*, and the Stoffel model in *b* and *e*. The surface areas were taken as listed in Table V.

TABLE VII
CALCULATED ISOELECTRIC POINTS OF MYELIN MEMBRANE SURFACES

Tissue or component	Surface			
	Cytoplasmic		Extracellular	
CNS				
protein (L; S)	11.4	11.5	7.0	10.7
PLP	10.4	9.8	7.0	10.7
MBP	11.7		—	
lipid	2.3		1.9	
net	9.3	9.1	2.4	3.2
PNS (+/+)				
protein	11.2		4.9	
P0	11.0		4.9	
MBP	11.7		—	
lipid	2.2		2.0	
net	9.0		4.0	
PNS (*shi/shi*)				
protein	11.0		4.9	
P0	11.0		4.9	
MBP	—		—	
lipid	2.2		2.0	
net	8.8		4.0	

L, Laursen model for PLP conformation (Laursen et al., 1984); S, Stoffel model for PLP (Stoffel et al., 1984). The isoelectric points were calculated at an ionic strength of 0.06. The surface areas of the models were from Table V.

myelins, especially at ionic strength 0.06. There was little disparity between the calculated and observed data at ionic strength 0.15 for PNS myelin in the range of pH 4–7.

The PNS myelin periods calculated as a function of ionic strength decreased monotonically with ionic strength at pH 7 (Fig. 4 *a*); however, the calculated values were larger than the observed ones. The calculation also did not reproduce the discontinuous compaction to the native period which was observed to occur at pH 7 and 9.7 when the ionic strength was >0.15 (Fig. 4 *a*).

At pH 4 the calculated periods for both PNS and CNS myelins should be constant whereas the measurements indicated an increase in period with ionic strength (Inouye and Kirschner, 1988). We found that reduction in the van der Waals attraction when the electrolyte concentration increases (Marra and Israelachvili, 1985; Marra, 1986) gave a closer fit between the calculated and observed values.

Reducing Surface Charge Improves Agreement with Measured Periods

The calculations based on our initial model correctly predicted the isoelectric points and characteristic shape (but not the magnitude) of the period versus pH and period versus ionic strength curves. Qualitatively, the increase in myelin period with pH and the decrease in period with ionic strength were consistent with an increasing amount of surface charge and a reduction in the screening effect of counterions, respectively. To obtain closer agreement between the calculated and the measured periods, it was clear that we had to reduce the electrostatic repulsion, i.e., reduce the surface charge density. We did this by introducing an adjustable parameter, λ, into the denominator of Eq. 1 and 4; with $\lambda > 1$, the charge density is reduced.

To determine an improved value for the surface charge density, we systematically increased the value of the product of λ and the surface area by increments of ~1,000 A^2 in Eq. 4, recalculated the surface potential (Eqs. 4 and 5), obtained the electrostatic repulsion force (Eq. 1 in accompanying paper), and recalculated the equilibrium period as a function of pH and ionic strength. Visual comparison of the calculated curve with the measurements indicated an improved value for the surface charge.

For PNS myelin at ionic strength 0.06, the calculated and observed periods were in close agreement both in the isoelectric range and above when the surface charge density was reduced by about fourfold for normal myelin and ~ threefold for shiverer myelin (Fig. 3) (i.e., λ ~4 and ~3, respectively). For PNS myelin at ionic strength 0.15, an improved fit was obtained when $\lambda \sim 0.6$. We found that λs could be plotted as a smooth function of ionic strength at different pH's (Fig. 4 *b*). This implies that the empirical parameter λ depends on the ionic strength but not on the pH. Thus, close agreement between the calculated and observed periods as a function of ionic strength could be achieved by using appropriate values for λS.

For CNS myelin at ionic strength 0.06, improved fits with the observed pH dependence data (Fig. 3) were obtained when the surface charge density was reduced by ~2.4 (using the Laursen model for PLP) or by ~1.5 (using the Stoffel model). The necessity to reduce the surface charge more with the Laursen model was due to a greater net negative charge density above the isoelectric range (see Fig. 2). We did not further examine the ionic strength dependence of myelin period in the CNS since the diffraction patterns showed indistinct, multiple phases at lower ionic strength.

DISCUSSION

Based on the known composition and localization of lipids and proteins in CNS and PNS myelins, we have determined the numbers and kinds of ionizable groups in the cytoplasmic and extracellular surfaces, and have calculated the charge density as a function of pH and ionic strength. The membrane separation calculated from such a distribution of charge as a function of pH is in agreement with the observed period in the isoelectric range, but above this range, the surface charge had to be reduced to obtain good agreement between calculated and observed periods, i.e., myelin composition gives a surface charge that predicts much greater electrostatic repulsion than is observed. We will first discuss what factors might explain this disparity, and then we will discuss how the myelin lipids and proteins and their localization can account for the

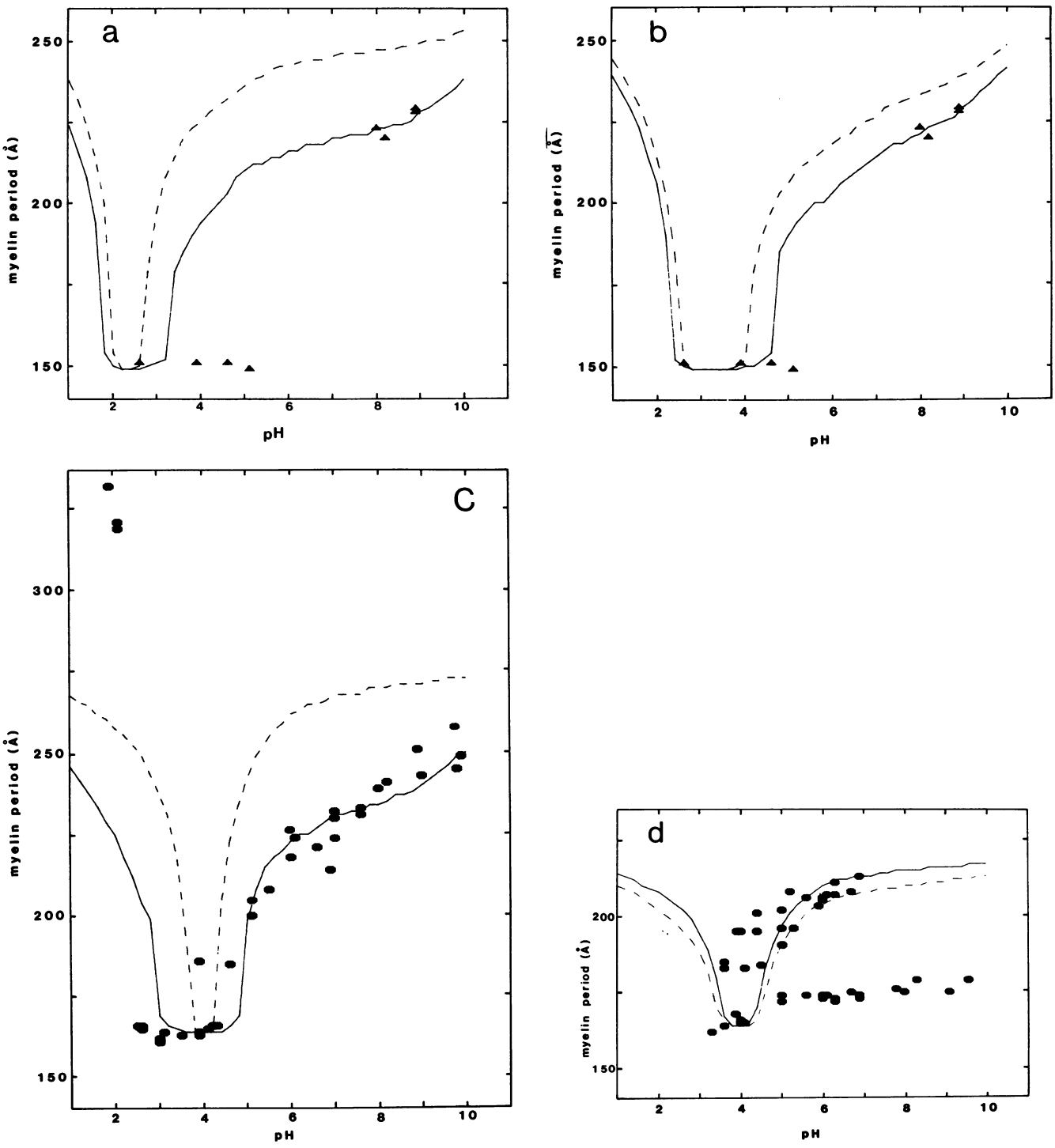

FIGURE 3 Calculated myelin period as a function of pH (at constant ionic strength 0.06 for *a–c*) for the initial models (*dashed lines*; $\lambda = 1$) and for the models with reduced surface charge densities (continuous curves). (*a*) CNS myelin, Laursen conformation for PLP. (*b*) CNS myelin, Stoffel conformation for PLP. (*c*) PNS myelin. (*d*) PNS myelin, ionic strength 0.15. The values of λ for the models with reduced charge densities were *a–c* 2.4, 1.5, and 4.3, respectively; and in *d* $\lambda = 0.6$. Apparent discontinuities in the continuous curves in this figure and in Fig. 4 *a* arise from round-off errors in the calculation.

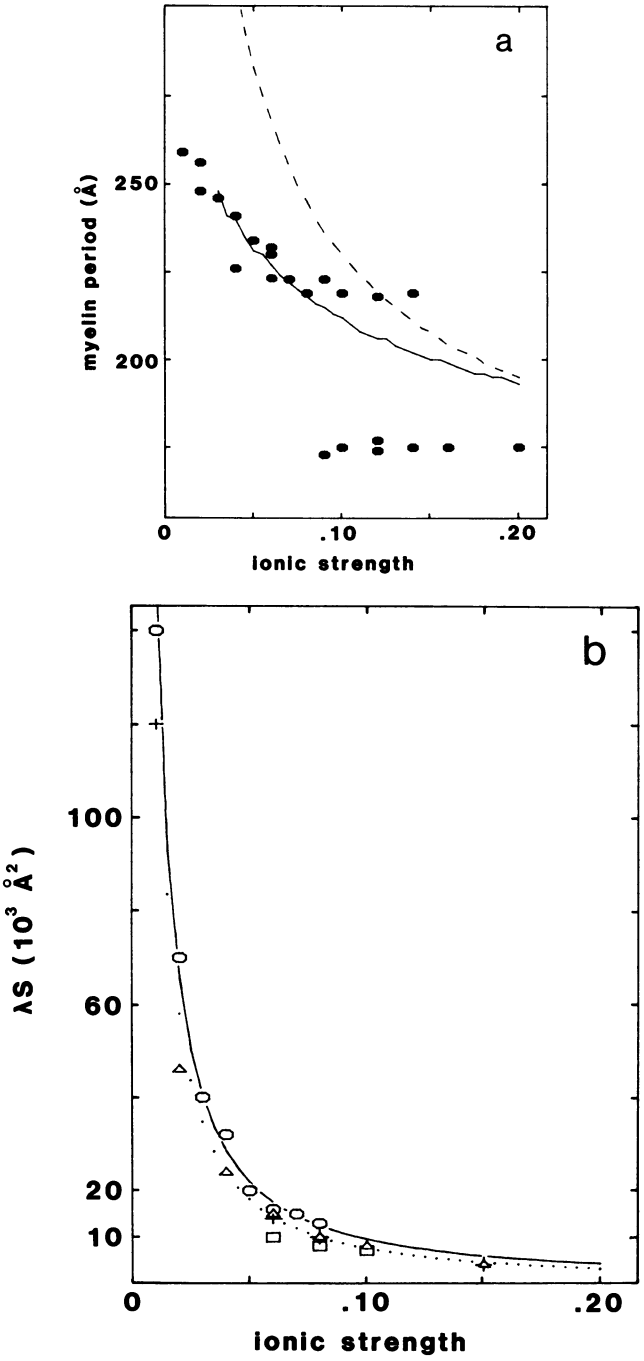

FIGURE 4 (*a*) Calculated period of PNS myelin as a function of ionic strength at constant pH 7. The large disparity between values calculated from the initial model (*dashed line*) and the observations (*data points*) was reduced by using a smaller surface charge density (*continuous curve*). (*b*) The effective surface area (λS) as a function of ionic strength at pH 5 (Δ), 6 (+), 7 (O), and 9.7 (□). The continuous curve was fit to the pH 7 data, and the dotted curve was fit to the four different pH data sets.

difference in inter-membrane interactions for the cytoplasmic versus extracellular appositions, and for CNS versus PNS myelin.

Physical Meaning of Reducing the Surface Charge Density

Several factors, singly or in combination, could account for the required lowering of the charge density: divalent cations binding to negatively charged residues; a space-charge rather than a planar-charge distribution in our calculation; a different chemical composition than we had used; and a hydrogen bonding effect on pK values. The first two possibilities will be discussed below. In recalculations that involved the binding of divalent cations or a space-charge approximation, we were able to obtain good agreement with the period versus pH data but not with the period versus ionic strength data. Similar disparities in comparing the calculated and observed ionic strength-dependency of charge have also been reported in other organized macromolecular systems (cited in accompanying paper, Inouye and Kirschner, 1988).

Divalent Cation Binding. If divalent cations bind to the negatively charged groups on the membrane surface (at pH > pI), then the surface charge (and the electrostatic potential and repulsion) is reduced. The extent of reduction depends on the binding constant and on the concentration of the divalent cations.

Assuming that the divalent cation binds to the negatively ionized group in a 1:1 stoichiometry, the concentration of the negatively charged group is

$$[A^-] = K_1[A]/([H_s^+] + K_1 + K_1K_2[M_s^{2+}]) \quad (8)$$

and the concentration of the positively charged group due to the binding of the divalent cation is

$$[AM^+] = K_1K_2[M_s^{2+}][A]/([H_s^+] + K_1 + K_1K_2[M_s^{2+}]), \quad (9)$$

where K_1 is the intrinsic proton dissociation constant of HA, K_2 is the intrinsic binding constant for A^- to M_s^{2+}, $[H_s^+]$ and $[M_s^{2+}]$ are the local concentrations of protons and divalent cations at the surface, and $[A] = [A^-] + [HA] + [AM^+]$. In this calculation the binding of the divalent cations to neutral groups was not considered. $[M_s^{2+}]$ is related to the bulk concentration of divalent cations $[M^{2+}]$ by the Boltzmann distribution.

$$[M_s^{2+}] = [M^{2+}] \exp[-2e\phi(x_s)/kT]. \quad (10)$$

We searched for agreement between the observed and calculated periods for PNS myelin at pH 4–9 and CNS myelin at pH 8–9 by systematically varying the parameter $K_2[M^{2+}]$ in increments of 0.005. The values for the surface areas and exclusion lengths were the same as in our initial model (Table V). Agreement was found using $K_2[M^{2+}]$ values of 0.02 (CNS, Laursen), 0.005 (CNS, Stoffel), 0.03 (PNS, normal myelin), and 0.02 (PNS, shiverer myelin).

How reasonable are these values? Assuming that $[M^{2+}]$ is 0.004 M, the physiological concentration of divalent cations, then the minimum and maximum values for K_2 are 1.2 M^{-1} and 7.5 M^{-1}. These are slightly less than the reported binding constants of calcium to phosphatidylcholine (10–$10^{2.5}$ M^{-1}, Rand, 1981; 21 M^{-1}, Ohshima et al., 1982), to phosphatidylcholine and phosphatidylethanolamine (12–120 M^{-1}, Marra and Israelachvili, 1985), and to phosphatidylserine (12 M^{-1}, McLaughlin et al., 1981). Although our bulk media did not contain any divalent cations, it is likely that there is endogenous calcium present in the tissue which strongly binds to the membranes (Pritchett and Rumsby et al., 1977; Moscarello et al., 1985).

Using our estimated binding constants, we also calculated the myelin period as a function of ionic strength (at constant pH 7) for normal and shiverer myelin. Although the calculated curve shifts slightly toward the observed curve, the disparity is still very large. Allowing the binding constant to depend on ionic strength would, of course, reduce the disparity. Also, the binding of anions at increased ionic strength could result in a greater repulsion than is calculated.

Space Charge Approximation. In calculating the electrostatic repulsion force we had assumed that the surface of the membrane was smooth and that all the ionizable groups were on the surface and were titratable. This assumption results in a greater surface charge density than if the surface of the membrane is allowed to have a finite thickness through which diffusable counterions can permeate. If ionizable groups are present throughout such a layer, which is termed a "fuzz coat" (Parsegian, 1974), then the surface potential at the front of this layer and the volume charge density not only depend on the electrolyte concentration and pH of the medium but also on the thickness and dielectric constant of the layer itself. When the Poisson-Boltzmann equation is linearized for the condition of a small surface potential, the volume charge density (σ_v) in the presence of a 1:1 electrolyte is given as

$$\sigma_v = e\phi(x_s)(2ne/kT)[\sinh(\kappa' d_f) + (\epsilon/\epsilon')^{1/2}\cosh(\kappa' d_f)]/\sinh(\kappa' d_f), \quad (11)$$

where κ' is the Debye parameter, ϵ' is the dielectric constant, and d_f is the thickness of the fuzz coat (Ohshima and Ohki, 1985). The volume charge density is written, similar to Eq. 1, as

$$\sigma_v = eN/(Sd_f). \quad (12)$$

Given ϵ' and d_f of the fuzz coat layer, and the pH and ionic composition of the medium, then ϕ_s and σ_v are obtained from these equations. The electrostatic potential at any point from the surface of the fuzz coat is given in the accompanying paper by Eq. 2. The myelin period is

$$d = d_w + d_{ex} + 2d_f, \quad (13)$$

where d_w is the partial thickness of the diffusable water, d_{ex} is the partial thickness of the exclusion layer which diffusable ions do not permeate, and d_f is the partial thickness of the fuzz coat layer. The distance between the charge fronts across the membrane pair is $d_{ex} + 2d_f$.

Values for d_f and ϵ' were assumed. We took the exclusion length as the distance between the extracellular lipid headgroup peaks across the pair of bilayers (see Table I in the accompanying paper). Given the closest approach of the two membranes for PNS and for CNS myelins, then d_f was 16 Å for PNS and 13 Å for CNS myelin. To prevent membranes from approaching more closely than their closest approach, we arbitrarily allowed the hydration type force to be extremely strong by assigning a decay constant of 0.1 and a magnitude of 1×10^{20} dyn/cm^2 (see Eq. 5 of accompanying paper). The best agreement between the calculated and observed periods as a function of pH (at ionic strength 0.06) was obtained by varying ϵ' while keeping the surface areas the same as in our initial model (Table V). For PNS myelin $\epsilon' \sim 5$, while for CNS myelin $\epsilon' \sim 10$ (using Laursen model for PLP) and ~53 (Stoffel model). Thus, inclusion of an apolar fuzz coat at the membrane surface can reduce substantially the electrostatic repulsion.

Using the coat layer specified as above the myelin periods were also calculated as a function of ionic strength. The period decreased with ionic strength as expected due to screening by the electrolytes in the diffusable layer. The estimates, however, were greater than the observed values at lower ionic strength and smaller at higher ionic strength.

It is clear that a joint effect of divalent cation binding with the space charge approximation would also reduce the electrostatic repulsion. Assuming that the surface potential at the front of the fuzz layer (Eq. 11) is constant through the layer, one would solve Eqs. 4, 8, 9, and 11 for the surface potential instead of using Eq. 5. In this calculation, assumptions would have to be made regarding values for the intrinsic binding constant of the divalent cations, and the dielectric constant and thickness of the fuzz layer.

Molecular Basis of Inter-Membrane Interactions in Myelin

The two membrane surfaces have opposite charge at neutral pH: at the cytoplasmic surface the isoelectric point is ~9, while at the extracellular surface pI ~ 2–4. Since the lipid contribution to the titration curve is similar for CNS and PNS myelins at both surfaces, then the opposite net charge at neutral pH is determined by the disposition of the proteins. The positive charge at the cytoplasmic surface is provided in CNS myelin by basic protein and PLP, and in PNS myelin by P0 glycoprotein and basic protein. The negative charge at the extracellular surface is due in the CNS to lipid and in the PNS to both P0 and lipid. The large number of acidic residues present in the proposed extracellular domain of P0 (Lemke and Axel, 1985) is thus

consistent with both the observed isoelectric point and the swelling property of PNS myelin. The suggestion that the negative charge at the extracellular apposition in CNS myelin arises largely from the lipid polar groups (Dermietzel et al., 1983) is consistent with our calculations which indicate only a minor contribution from PLP at this surface. In addition, our data substantiates localization of basic protein to the cytoplasmic apposition since models which place basic protein at the extracellular apposition give a calculated pI of 9.3 in the CNS and 5.3 in the PNS, values that are not in agreement with the observations.

As illustrated by the hydropathic profiles and charge distribution curves (Fig. 1) two conformations for PLP in the membrane have been suggested (Laursen et al., 1984; Stoffel et al., 1984). In the Laursen model the hydrophilic cluster which is largely composed of basic residues is assigned to the cytoplasmic surface, whereas in the Stoffel model this positively charged domain is assigned to the extracellular surface. As a result, above the isoelectric range the net charge density at the extracellular surface is less negative with the Stoffel PLP model than with the Laursen model, and less electrostatic repulsion and smaller myelin periods were calculated using the Stoffel model. Therefore, our observed pH-dependence of the myelin periods (at ionic strength 0.06) favors the Stoffel model over the Laursen model for the conformation of PLP.

Role of Proteins and Lipids in Inter-Membrane Interactions

CNS Myelin. The lack of ordered swelling in the range of pH 5–8 may be due to the projection of hydrophobic, extracellular domains of PLP into the apposing membrane bilayer. The notion that PLP promotes adhesion of myelin membrane bilayers by such a mechanism has been proposed from the postulated conformations of PLP (Laursen et al., 1984; Stoffel et al., 1985). Above pH 8–9 the electrostatic repulsion, which is due primarily to the lipids, may be sufficient to overcome the hydrophobic interactions so that the membrane pairs can achieve an ordered swollen arrangement.

PNS Myelin. The native-period structure was observed only at neutral or slightly higher pH at ionic strength ~0.15. At acidic pH and ionic strength 0.15 the myelin swelled to periods almost as large as those at lower ionic strength 0.06; however, above pH 7 the period abruptly compacted to the native period. This discontinuous transition, which is not apparent from the model, suggests that some conformational change occurs at this pH and ionic strength which energetically overwhelms the very appreciable electrostatic repulsion. We suggest that the three histidine residues which are postulated to be in the extracellular domain of P0 (Lemke and Axel, 1985) and which have pK ~ 6.0 (Nozaki and Tanford, 1967) may be involved in this conformational change. Loss of positive charge from the imidazole groups of the histidines could cause an increase in hydrophobic attraction at the extracellular boundary.

Are the energetics favorable for a hydrophobic-driven compaction from swollen myelin? We have estimated the energy of this transition by comparing the difference in energy between the 230 Å-period and the 165 Å-period structures (since native periods could never be calculated from the model). The potential energy minima for these structures are -1×10^{-3} erg/cm^2 and -10×10^{-3} erg/cm^2, respectively (Fig. 10 in the accompanying paper, Inouye and Kirschner, 1988); so the difference in energy in going from the swollen to the compact membrane array (for a membrane surface area of ~4,000 Å^2 containing one P0 molecule; see Table V) is -4×10^{-15} erg = -0.4×10^{-24} kJ. A hydrophobic interaction involving, for example, the transfer of one methyl group to a nonpolar environment, would provide a free energy of $\sim 10 \times 10^{-24}$ kJ/molecule (Tanford, 1980) which is substantially more than needed to fuel the compaction. Since there are many hydrophobic residues in the extracellular domain of P0 (Lemke and Axel, 1985; see also Fig. 1) it is quite possible that hydrophobic interactions between these groups could occur and could provide sufficient energy for the transition from the swollen to the native-period structure. The conformational modification of the protein must be very specific since the transition occurs over a relatively limited range of ionic strength and pH.

The compact-period array obtained after prolonged incubation in distilled water (Inouye and Kirschner, 1988) was similar to the one obtained in the isoelectric range, indicating that the membrane surfaces have, with time, developed a zero net surface charge in the absence of counterions. Since the compact phase reversed to the swollen phase when only 1 mM concentration of counterions was restored, it is unlikely that chemical modification of negatively-charged groups can account for the anomalous compaction. Rather, the transition may occur as a result both of neutralizing interactions between negatively-charged lipids and positively-charged amino acid residues of P0 glycoprotein, and also hydrophobic interactions involving P0. Shiverer myelin showed compaction sooner than normal myelin, suggesting that the absence of basic protein from the cytoplasmic side of the membrane might increase the conformational flexibility of the transmembrane P0 in the extracellular half (Inouye and Kirschner, 1984).

Specific Interactions Dominate the Cytoplasmic Apposition

In contrast to the extracellular apposition at which nonspecific forces account for much of the interactions between the membranes, the invariance of the cytoplasmic separation over a wide range of pH and ionic strength indicates a dominance of specific, short-range interactions. The relative invariance of this apposition is particularly remarkable

when one considers that the surface charge, calculated from the biochemical composition and localization data, is strongly positive at neutral pH. Our data suggest that if either basic protein, PLP or P0 interacts with negatively-charged acidic lipids in the cytoplasmic leaflet (Rumsby and Crang, 1977), then the ion pairs of such an interaction are not readily accessible to the changes in pH and ionic strength of our bathing medium. Since proteins are highly permeable across lipid bilayers and membranes (Gutknecht, 1984; Deamer and Bramhall, 1986), this explanation may be unlikely. Rather, hydrophobic interactions may underlie the stability at the cytoplasmic apposition. By virtue of their abundance, basic protein in the CNS and P0 in the PNS are the most likely proteins involved in such an interaction.

CONCLUSIONS

Uncertainties in the composition of myelin and in the localization of its molecular components make it difficult to calculate with complete confidence the charge density on the two membrane leaflets. Nevertheless, our analysis shows that current ideas about myelin biochemical architecture are in fact quite consistent with the x-ray structural measurements on myelin of intact tissue; however, a better comparison might be made by using isolated myelin itself for the diffraction measurements at different pH and ionic strength (Karthigasan and Kirschner, 1988). While non-specific forces can account for much of the extracellular interactions, further information about the specific interactions underlying certain conformation changes at the extracellular apposition and the invariant spacing at the cytoplasmic apposition will of necessity derive from x-ray crystallographic determinations of the three-dimensional structure of myelin proteins.

We are grateful to Drs. V. Adrian Parsegian and Barry M. Millman for invaluable comments on the manuscript. This research was supported by National Institutes of Health grants NS-20824 (to Daniel A. Kirschner) from the National Institute of Neurological and Communicative Disorders and Stroke. This work was carried out in facilities of the Mental Retardation Research Center which is supported by National Institutes of Health core grant HD-06276.

Received for publication 27 May 1987 and in final form 25 September 1987.

REFERENCES

Allt, G., C. E. Blanchard, M. L. MacKenzie, and K. Sikri. 1985. Distribution of filipin-sterol complexes in the myelinated nerve fiber. *J. Ultrastruct. Res.* 91:104–111.

Althaus, H.-H., S. Klöppner, H-M. Poehling, and V. Neuhoff. 1983. Two-dimensional gel electrophoresis of myelin and oligodendroglial proteins solubilized by a mixture of tetramethylurea and dimethylethylene urea. *Electrophoresis.* 4:347–353.

Barbarese, E., J. H. Carson, and P. E. Braun. 1978. Accumulation of the four myelin basic proteins in mouse brain during development. *J. Neurochem.* 31:779–782.

Carnegie, P. R., and W. J. Moore. 1980. Myelin basic protein. *In* Properties of the Nervous System. Bradshaw, R. A., and D. M. Schneider, editors), pp. 119–143. Raven Press, New York.

Caspar, D. L. D., and D. A. Kirschner. 1971. Myelin membrane structure at 10 Å resolution. *Nature (Lond.).* 231:46–52.

Cevc, G., A. Watts, and D. Marsh. 1981. Titration of the phase transition of phosphatidylserine bilayer membranes: effects of pH, surface electrostatics, ion binding, and head-group hydration. *Biochemistry.* 20:4955–4965.

Deamer, D. W., and J. Bramhall. 1986. Permeability of lipid bilayers to water and ionic solutes. *Chem. Phys. Lipids.* 40:167–188.

Dermietzel, R., N. Thürauf, and D. Schünke. 1983. Cytochemical demonstration of negative surface charges in central myelin. *Brain Res.* 262:225–232.

Draper, M., M. B. Lees, and D. S. Chan. 1978. Isoelectric focusing of proteolipid. *J. Neurochem.* 31:1095–1099.

Eisenberg, D., E. Schwarz, M. Komaromy, and R. Wall. 1984. Analysis of membrane and surface protein sequences with the hydrophobic moment plot. *J. Mol. Biol.* 179:125–142.

Feinstein, M. B., and H. Felsenfeld. 1975. Reactions of fluorescent probes with normal and chemically modified myelin basic protein and proteolipid. Comparisons with myelin. *Biochemistry.* 14:3049–3056.

Finean, J. B. 1957. The role of water in the structure of peripheral nerve myelin. *J. Biophys. Biochem. Cytol.* 3:95–102.

Greenfield, S., S. Brostoff, E. H. Eylar, and P. Morell. 1973. Protein composition of myelin of the peripheral nervous system. *J. Neurochem.* 20:1207–1216.

Greenfield, S., S. W. Brostoff, and E. L. Hogan. 1980. Characterization of the basic proteins from rodent peripheral nervous system myelin. *J. Neurochem.* 34:453–455.

Greenfield, S., W. T. Norton, and P. Morell. 1971. Quaking mouse: isolation and characterization of myelin protein. *J. Neurochem.* 18:2119–2128.

Gutknecht, J. 1984. Proton/hydroxide conductance through lipid bilayer membranes. *J. Membrane Biol.* 82:105-112.

Gwarsha, K., M. G. Rumsby, and C. Little. 1984. On the disposition of phospholipids in freshly isolated myelin sheath preparations from bovine brain. *Neurochem. Int.* 6:599–606.

Inouye, H., and D. A. Kirschner. 1984. Effects of $ZnCl_2$ on membrane interactions in myelin of normal and shiverer mice. *Biochim. Biophys. Acta.* 776:197–208.

Inouye, H., and D. A. Kirschner. 1986a. Myelin membrane structure modeled to account for pH titration curves. *Trans. Am. Soc. Neurochem.* 17:156.

Inouye, H., and D. A. Kirschner. 1986b. Modeling the extracellular and cytoplasmic surfaces of myelin from x-ray diffraction studies of membrane interactions. *Amer. Crystall. Assoc. Annu. Mtg.* 14:44.

Inouye, H., and D. A. Kirschner. 1988. Membrane interactions in nerve myelin: I. Determination of surface charge from effects of pH and ionic strength on period. *Biophys. J.* 53:00–00.

Inouye, H., A. L. Ganser, and D. A. Kirschner. 1985. Shiverer and normal peripheral myelin compared: basic protein localization, membrane interactions and lipid composition. *J. Neurochem.* 45:1911–1922.

Ishaque, A., M. W. Roomi, I. Szymanska, S. Kowalski, and E. H. Eylar. 1980. The P0 glycoprotein of peripheral nerve myelin. *Can. J. Biochem.* 58:913–921.

Karthigasan, J., and D. A. Kirschner. 1987. Membrane interactions in isolated myelin. *J. Neurochem.* 48:5134.

Kirschner, D. A., and D. L. D. Caspar. 1975. Myelin structure transformed by dimethylsulfoxide. *Proc. Natl. Acad. Sci. USA.* 72:3513–3517.

Kirschner, D. A., and A. L. Ganser. 1982. Myelin labeled with mercuric chloride: asymmetric localization of phosphatidylethanolamine plasmalogen. *J. Mol. Biol.* 157:635–658.

Kirschner, D. A., A. L. Ganser, and D. L. D. Caspar. 1984. Diffraction studies of molecular organization and membrane interactions in mye-

lin. *In* Myelin. Morell, P., editor. pp 51–95. Plenum Publishing Co., New York.

Kitamura, K., M. Suzuki, A. Suzuki, and K. Uyemura. 1980. The complete amino acid sequence of the P2 protein in bovine peripheral nerve myelin. FEBS (*Fed. Eur. Biochem. Soc.*) Lett. 115:27–30.

Laursen, R. A., M. Samiullah, and M. B. Lees. 1984. The structure of bovine brain proteolipid and its organization in myelin. *Proc. Natl. Acad. Sci. USA.* 81:2912–2916.

Lees, M. B., and S. W. Brostoff. 1984. Proteins in myelin. *In* Myelin. Morell, P., editor. pp. 197–224. Plenum Publishing Co., New York. 197–224.

Lemke, G., and R. Axel. 1985. Isolation and sequence of a cDNA encoding the major structural protein of peripheral myelin. *Cell.* 40:501–508.

Linington, C., and M. G. Rumsby. 1980. Accessibility of galactosylceramides to probe reagents in central nervous system myelin. *J. Neurochem.* 35:983–992.

Linington, C., T. V. Waehneldt, and V. Neuhoff. 1980. The lipid composition of light and heavy myelin subfractions isolated from rabbit sciatic nerve. Neuroscience *Lett.* 20:211–215.

Marra, J. 1986. Direct measurements of attractive van der Waals and adhesion forces between uncharged lipid bilayers in aqueous solutions. *J. Colloid Interface Sci.* 109:11–20.

Marra, J., and J. Israelachvili. 1985. Direct measurements of forces between phosphatidylcholine and phosphatidylethanolamine bilayers in aqueous electrolyte solutions. *Biochemistry.* 24:4608–4618.

Matthieu, J.-M., T. V. Waehneldt, H. deF. Webster, M. Bény, and G. Fagg. 1979. Distribution of PNS myelin proteins and membrane enzymes in fractions isolated by continuous gradient zonal centrifugation. *Brain Res.* 170:123–133.

McLaughlin, S., N. Mulrine, T. Gresalfi, G. Vaio, and A. McLaughlin. 1981. Adsorption of divalent cations to bilayer membranes containing phosphatidylserine. *J. Gen. Physiol.* 77:445–473.

Micko, S., and W. W. Schlaepfer. 1978. Protein composition of axons and myelin from rat and human peripheral nerves. *J. Neurochem.* 30:1041–1049.

Milner, R. J., C. Lai, K-A. Nave, D. Lenoir, J. Ogata, and J. G. Sutcliffe. 1985. Nucleotide sequences of two mRNAs for rat brain myelin proteolipid protein. *Cell.* 42:931–939.

Morell, P., S. Greenfield, E. Constantino-Ceccarini, and H. Wisniewski. 1972. Changes in the protein composition of mouse brain myelin during development. *J. Neurochem.* 19:2545–2554.

Morell, P., R. Lipkind, and S. Greenfield. 1973. Protein composition of myelin from brain and spinal cord of several species. *Brain Res.* 58:510–514.

Moscarello, M. A., L.-S. Chia, D. Leighton, and D. Absolom. 1985. Size and surface charge properties of myelin vesicles from normal and diseased (multiple sclerosis) brain. *J. Neurochem.* 45:415–421.

Ninham, B. W., and V. A. Parsegian. 1971. Electrostatic potential between surfaces bearing ionizable groups in ionic equilibrium with physiologic saline solution. *J. Theor. Biol.* 31:405–428.

Norton, W. T., and W. Cammer. 1984. Isolation and characterization of myelin. *In* Myelin. Morell, P., editor. pp. 147–195. Plenum Publishing Co., New York.

Nozaki, Y., and C. Tanford. 1967. Examination of titration behavior. *Methods Emzymol.* 11:715–734.

Nunn, D. J., and C. Mezei. 1984. Solid-phase immunoassay of P0 glycoprotein peripheral nerve myelin. *J. Neurochem.* 42:158–165.

O'Brien, J. S., and E. L. Sampson. 1965. Lipid composition of the normal human brain: gray matter, white matter and myelin. *J. Lipid Res.* 6:537–544.

Ohshima, H., and S. Ohki. 1985. Donnan potential and surface potential of a charged membrane. *Biophys. J.* 47:673–678.

Ohshima, H., Y. Inoko, and T. Mitsui. 1982. Hamaker constant and binding constants of Ca^{2+} and Mg^{2+} in dipalmitoyl phosphatidylcholine/water system. *J. Colloid Interface Sci.* 86:57–72.

Parsegian, V. A. 1974. Possible modulation of reactions on the cell surface by changes in electrostatic potential that accompany cell contact. *Ann. N. Y. Acad. Sci.* 238:362–371.

Pritchett, S. M., and M. G. Rumsby. 1977. Development and application of method to assay calcium and magnesium in isolated myelin sheath preparations. *Biochem. Soc. Trans.* 5:1429–1431.

Quarles, R. H., G. R. Barbarash, D. A. Figlewicz, and L. J. McIntyre. 1983. Purification and partial characterization of the myelin-associated glycoprotein from adult rat brain. *Biochim. Biophys. Acta* 757:140–143.

Rand, R. P. 1981. Interacting phospholipid bilayers: measured forces and induced structural changes. *Ann. Rev. Biophys. Bioeng.* 10:277–314.

Rumsby, M. G., and A. J. Crang. 1977. The myelin sheath–a structural examination. *In* The Synthesis, Assembly and Turnover of Cell Surface Components. Poste, G., and G. L. Nicolson, editors. pp. 247–362. Elsevier/North-Holland Biomedical Press, Amsterdam.

Sacré, M. M., and J. F. Tocanne. 1977. Importance of glycerol and fatty acid residues on the ionic properties of phosphatidylglycerols at the air-water interface. *Chem. Phys. Lipids.* 18:334–354.

Schmitt, F. O., R. S. Bear, and K. J. Palmer. 1941. X-ray diffraction studies on the structure of the nerve myelin sheath. *J. Cell. Comp. Physiol.* 18:31–42.

Scott, S. C., K. R. Bruckdorfer, and D. L. Worcester. 1980. The symmetrical distribution of cholesterol across the myelin membrane bilayer determined by deuterium labelling in vivo and neutron diffraction. *Biochem. Soc. Trans.* 8:717.

Seimiya, T., and S. Ohki. 1973. Ionic structure of phospholipid membranes, and binding of calcium ions. *Biochim. Biophys. Acta.* 298:546–561.

Smith, M. E. 1968. The turnover of myelin in the adult rat. *Biochim. Biophys. Acta.* 164:285–293.

Smith, M. E., and B. M. Curtis. 1979. Frog sciatic nerve myelin: a chemical characterization. *J. Neurochem.* 33:447–452.

Stoffel, W., H. Giersiefen, H. Hillen, W. Schroeder, and B. Tunggal. 1985. Amino-acid sequence of human and bovine brain myelin proteolipid protein (Lipophilin) is completely conserved. *Biol. Chem. Hoppe-Seyler.* 366:627–635.

Stoffel, W., H. Hillen, and H. Giersiefen. 1984. Structure and molecular arrangement of proteolipid protein of central nervous system myelin. *Proc. Natl. Acad. Sci. USA.* 81:5012–5016.

Tanford, C. 1980. The Hydrophobic Effect. John Wiley and Sons, Inc., New York.

Thomas, C., and L. Ter Minassian-Saraga. 1976. Characterization of monolayers of a structural protein from myelin spread at the air/water interface. Effects of pH and ionic strength. *J. Colloid Interface Sci.* 56:412–425.

Trapp, B. D., R. H. Quarles, and K. Suzuki. 1984. Immunocytochemical studies of quaking mice support a role for the myelin-associated glycoprotein in forming and maintaining the periaxonal space and periaxonal cytoplasmic collar of myelinating Schwann cells. *J. Cell Biol.* 99:594–606.

Trotter, J. L., L. Lieberman, F. L. Margolis, and H. C. Agrawal. 1981. Radioimmunoassay for central nervous system myelin-specific proteolipid protein. *J. Neurochem.* 36:1256–1262.

Verwey, E. J. W., and J. Th. G. Overbeek. 1948. Theory of the Stability of Lyophobic Colloids. Elsevier, New York.

Waehneldt, T. V. 1978. Density and protein profiles of myelin from two regions of young and adult rat CNS. *Brain Res. Bull.* 3:37–44.

Webster, H. deF., C. G. Palkovits, G. L. Stoner, J. T. Favilla, D. E. Frail, and P. E. Braun. 1983. Myelin-associated glycoprotein: electron microscopic immunocytochemical localization in compact developing and adult central nervous system myelin. *J. Neurochem.* 41:1469–1479.

Weise, M. J. 1985. Hydrophobic regions in myelin proteins characterized through analysis of "hydropathic" profiles. *J. Neurochem.* 44:163–170.

Weise, M. J., S. Greenfield, S. W. Brostoff, and E. L. Hogan. 1983.

Protein composition of PNS myelin: developmental comparison of control and quaking mice. *J. Neurochem.* 41:448–453.

Wiggins, R. C., J. A. Benjamins, and P. Morell. 1975. Appearance of myelin proteins in rat sciatic nerve during development. *Brain Res.* 89:99–106.

Worthington, C. R. 1971. X-ray analysis of nerve myelin. *In* Biophysics and Physiology of Excitable Membranes. Adelman, W. J., Jr., editor. pp. 1–46. Van Nostrand Reinhold Co., Inc., New York.

Zgorzalewicz, B., V. Neuhoff, and T. V. Waehneldt. 1974. Rat myelin proteins: compositional changes in various regions of the nervous system during ontogenetic development. *Neurobiology (Copenh.).* 4:265–276.